

Likelihood Variance as Text Importance for Resampling Texts to Map Language Models

Momose Oyama^{1,2} Ryo Kishino¹ Hiroaki Yamagiwa¹ Hidetoshi Shimodaira^{1,2}

¹Kyoto University ²RIKEN

oyama.momose@sys.i.kyoto-u.ac.jp, kishino.ryo.32s@st.kyoto-u.ac.jp

{h.yamagiwa, shimo}@i.kyoto-u.ac.jp

Abstract

We address the computational cost of constructing a model map, which embeds diverse language models into a common space for comparison via KL divergence. The map relies on log-likelihoods over a large text set, making the cost proportional to the number of texts. To reduce this cost, we propose a resampling method that selects important texts with weights proportional to the variance of log-likelihoods across models for each text. Our method significantly reduces the number of required texts while preserving the accuracy of KL divergence estimates. Experiments show that it achieves comparable performance to uniform sampling with about half as many texts, and also facilitates efficient incorporation of new models into an existing map. These results enable scalable and efficient construction of language model maps.

1 Introduction

For the systematic comparison of numerous language models, Oyama et al. (2025) proposed a method to estimate Kullback-Leibler (KL) divergence between language models based on log-likelihood vectors. In this method, language models with different architectures are embedded into a common space, and visualizing this creates a map of language models (Fig. 1).

The model map is constructed using a text set $D_N = \{x_1, \dots, x_N\}$. Since D_N is a sample from a broader text population $D^\dagger = \{x_1^\dagger, \dots, x_{N_0}^\dagger\}$, it introduces sampling error relative to the true relationships between models in the population¹. Additionally, the computational cost, which is proportional to the number of texts N , is also an issue.

To reduce computational costs for adding new models to the map, we consider resampling n texts from the data D_N with replacement, and then reconstruct the model map using the resulting set

¹When the entire Pile corpus is converted into 1,024-byte text chunks, the total number of texts is $N_0 = 5,703,791$.

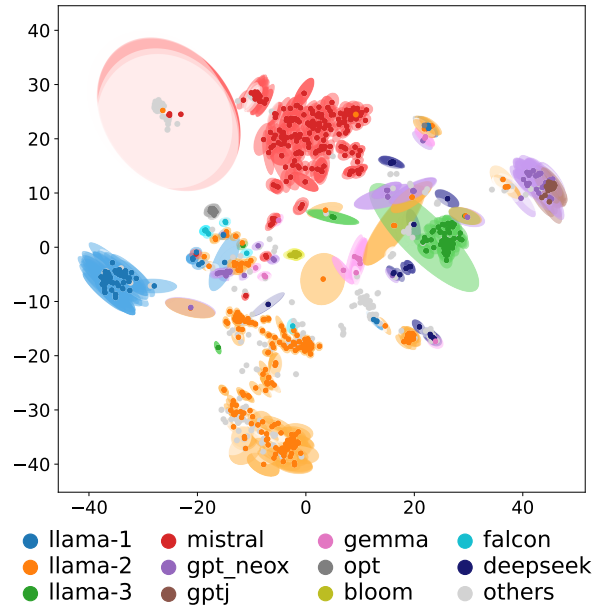


Figure 1: The model map calculated with D_N is visualized using t-SNE. The sampling error for each point was estimated using the bootstrap resampling method and shown as an ellipse. See Appendix B for details.

D_d^* of d unique texts ($d \leq n$). When we discuss the distance between models calculated using log-likelihood vectors and the reliability of the model map, it is crucial to focus on the sampling error with respect to the population.

To estimate the resampling error of the distance between models measured based on D_d^* relative to the true distances in the population, two types of errors need to be considered. The first is the **sampling error** that the original data D_N has with respect to the population D^\dagger , and the second is the **resampling error** incurred when selecting D_d^* from D_N .

Since uniform resampling from data D_N has limitations, we propose a method to resample important texts with high probability. This idea is based on the column sampling method of Drineas and Kannan (2001), which was originally proposed

for approximating matrix products. Through experiments, we show that our proposed text resampling method achieves comparable estimation error to uniform random sampling with about half the number of texts, and is also effective when adding new models to an existing model map.

2 Background

2.1 Map of Language Models

The map of K language models p_1, \dots, p_K is constructed based on a text set $D_N = \{x_1, \dots, x_N\}$. The log-likelihood of model p_i for text x_s is denoted by $\log p_i(x_s)$, and the log-likelihood matrix $L \in \mathbb{R}^{K \times N}$ is composed of these elements. Let $Q \in \mathbb{R}^{K \times N}$ be the matrix obtained by applying double centering² to matrix L . The i -th row vector $q_i \in \mathbb{R}^N$ of this matrix serves as the coordinate for language model p_i . Oyama et al. (2025) showed that the KL divergence between models p_i and p_j can be estimated by the following equation:

$$2 \text{KL}(p_i, p_j) \approx \|q_i - q_j\|^2 / N.$$

2.2 Length Squared Sampling

The idea of resampling text based on its importance is derived from column sampling methods, which probabilistically select a small number of columns from a matrix $A = (A^{(1)}, \dots, A^{(N)}) \in \mathbb{R}^{K \times N}$ to approximate the matrix product AA^\top .

In the representative Length Squared (LS) sampling method (Drineas and Kannan, 2001), each column $A^{(s)}$ is sampled with a probability proportional to the square of its Euclidean norm, $\|A^{(s)}\|^2$. This is known to minimize the expected Frobenius norm of the approximation error for AA^\top .

3 Resampling Texts for Model Map

3.1 Text Resampling Method

We apply the idea of LS sampling to reduce the number of texts used for the model map, while estimating the model distance $\|q_i - q_j\|^2$ as accurately as possible. To determine the probability π_s that text x_s is resampled from dataset $D_N = \{x_1, \dots, x_N\}$, we utilize the information in the double centered log-likelihood matrix $Q \in \mathbb{R}^{K \times N}$.

LS Sampling. Following Drineas and Kannan (2001), we set $\pi_s \propto \|Q^{(s)}\|^2$. The squared norm

²Centering is performed row-wise (per model) and then column-wise (per text).

$\|Q^{(s)}\|^2$ corresponds to the variance of the log-likelihoods for text x_s across models. This is optimal for approximating the inner product $q_i^\top q_j$, but not necessarily optimal for our goal of approximating the squared Euclidean distance $\|q_i - q_j\|^2$.

KL Sampling. Therefore, we aim to directly minimize the estimation error of the squared Euclidean distance and propose KL sampling, where

$$\pi_s \propto \sqrt{\sum_{i,j=1}^K (q_i(x_s) - q_j(x_s))^4}.$$

Here, $q_i(x_s)$ represents the (i, s) -th component of matrix $Q \in \mathbb{R}^{K \times N}$. We show in Appendix C that this method yields an optimal approximation of the squared Euclidean distance $\|q_i - q_j\|^2$.

Baseline: Uniform Sampling. All texts are resampled with equal probability $\pi_s = 1/N$.

3.2 Model Map with Resampled Texts

Let \tilde{D}_n be the dataset obtained by resampling n texts from D_N , and the set of d unique texts in \tilde{D}_n be $D_d^* = \{x_{u_1}, \dots, x_{u_d}\}$. We denote $c(u_t)$ as the number of times each text x_{u_t} was resampled, such that $\sum_{t=1}^d c(u_t) = n$.

We construct the log-likelihood matrix $L_d \in \mathbb{R}^{K \times d}$ using the d resampled texts and obtain \tilde{Q}_d by double centering. In row-wise centering, the column $L^{(u_t)}$ corresponding to the resampled text x_{u_t} is weighted by $w_{u_t} = c(u_t)/n\pi_{u_t}$, based on the resampling probability π_s and the number of times it was resampled $c(u_t)$. Let $\tilde{q}_i \in \mathbb{R}^d$ be the row vector of \tilde{Q}_d . The distance of model p_i and p_j is calculated by the squared Euclidean distance using weights $w_d = (w_{u_1}, \dots, w_{u_d})$:

$$\|\tilde{q}_i - \tilde{q}_j\|_{w_d}^2 := \sum_{t=1}^d \frac{c(u_t)}{n\pi_{u_t}} (\tilde{q}_i(x_{u_t}) - \tilde{q}_j(x_{u_t}))^2.$$

Here, $\tilde{q}_i(x_{u_t})$ is the (i, t) -th component of matrix $\tilde{Q}_d \in \mathbb{R}^{K \times d}$.

4 Experiments

4.1 Error of Resampled Estimates

The dataset D_N is a random sample from the text population D^\dagger , and \tilde{D}_n is resampled dataset from D_N . The squared Euclidean distances computed from D^\dagger , D_N , and \tilde{D}_n are, respectively, $g_{ij}^\dagger = (N/N_0)\|q_i^\dagger - q_j^\dagger\|^2$, $g_{ij} = \|q_i - q_j\|^2$,

$\tilde{g}_{ij} = \|\tilde{\mathbf{q}}_i - \tilde{\mathbf{q}}_j\|_{w_d}^2$ where the scaling ensures comparability across different dimensionalities³.

Our objective is to evaluate the error, which is how much \tilde{g}_{ij} deviates from the unknown true value g_{ij}^\dagger in the population. Since $N_0 \gg N$, g_{ij}^\dagger is difficult to compute, so we estimate the error using D_N . Details on the error estimation method are described in Appendix E.

Resampling Error to Population ($\hat{\sigma}_{\text{Method},n}$). Let $\hat{\sigma}_{\text{Method},n}$ (Method $\in \{\text{LS}, \text{KL}, \text{unif}\}$) be the estimated error relative to the true value g_{ij}^\dagger in the population D^\dagger . This is estimated by considering the following two errors:

$$\hat{\sigma}_{\text{Method},n} = \sqrt{\tau_{\text{unif},N}^2 + \tau_{\text{Method},n}^2}$$

Here, $\tau_{\text{unif},N}$ is the bootstrap estimate (Efron and Tibshirani, 1994) of the sampling error that D_N itself has with respect to the population D^\dagger . $\tau_{\text{Method},n} = \sqrt{\tau_{\text{Method},n}^2}$ is the Root Mean Squared Error (RMSE) of resampling (Method) with respect to D_N , and it is calculated from the aggregated MSE of the relative error $\tilde{e}_{ij} = (\tilde{g}_{ij} - g_{ij})/\max(g_{ij}, \varepsilon_0)$ as $\tau_n^2 = \frac{1}{K^2 R} \sum_{i,j=1}^K \sum_{r=1}^R (\tilde{e}_{ij}^{(r)})^2$. In the experiments, we set $\varepsilon_0 = 10^{-3}$, $R = 100$, and varied n from 10 to 10,000.

Baseline: Sampling Error ($\hat{\kappa}_m$). Let κ_m be the aggregated relative error of g_{ij} with respect to the true value g_{ij}^\dagger in the population. In this sampling, all m texts are unique, so the number of unique texts is $d = m$. The bootstrap estimate (Efron and Tibshirani, 1994) of κ_m is $\hat{\kappa}_m = \tau_{\text{unif},m}$.

Results. Figure 2 shows the relationship between the number of unique texts d and the estimated error with respect to the population for each resampling method. The dotted line represents the estimated error $\hat{\kappa}_d$ when d texts are directly randomly sampled from the population D^\dagger , and the thick gray solid line shows its theoretical value, computed as $\sqrt{N/d} \hat{\kappa}_N$. The colored solid lines represent the estimated error $\hat{\sigma}_{\text{Method},n}$ when resampling from D_N using each method. Comparing the blue solid line (Uniform resampling from D_N) and the black dotted line (direct sampling from D^\dagger), Uniform resampling from D_N results in an error comparable to directly sampling the same number of texts from

³The coordinate of p_i in D^\dagger is denoted by $\mathbf{q}_i^\dagger \in \mathbb{R}^{N_0}$. g_{ij}^\dagger and \tilde{g}_{ij} are scaled to match g_{ij} .

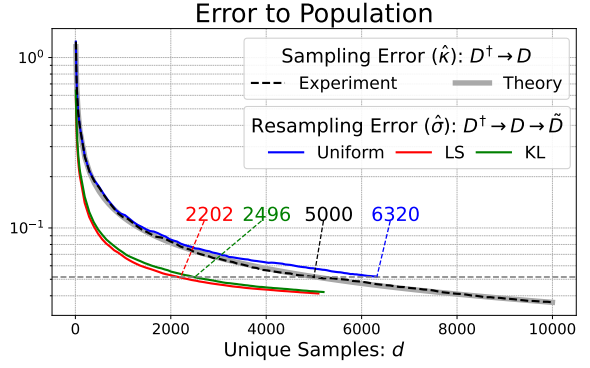


Figure 2: The number of unique texts d for each resampling method and the estimation error against the population. ‘Sampling Error’ corresponds to the estimation error when d texts are randomly sampled without replacement from the population D^\dagger . Here, the error is normalized by KL divergence for each model pair. For error evaluation without normalization, see Appendix D.

| m | 500 | 2,500 | 5,000 | 7,500 |
|---------|-------------|----------------|----------------|----------------|
| Uniform | 582 ± 4 | $2,877 \pm 18$ | N/A | N/A |
| KL | 196 ± 2 | $1,070 \pm 10$ | $2,496 \pm 22$ | $4,780 \pm 33$ |
| LS | 195 ± 2 | 895 ± 8 | $2,202 \pm 19$ | $4,229 \pm 30$ |

Table 1: Average and standard deviation of the number of unique texts d in resampled dataset \tilde{D}_n , where n is the smallest value satisfying $\hat{\sigma}_{\text{Method},n} \leq \hat{\kappa}_m$.

the population⁴. In contrast, LS sampling and KL sampling achieve an error comparable to the estimated error $\hat{\kappa}_d$ of random sampling d texts from the population with a smaller number of unique texts. As can be seen from Table 1, an error comparable to $\hat{\kappa}_{5,000}$ is achieved with LS sampling using an average of $d = 2,202$ texts, and with KL sampling using an average of $d = 2,496$ texts, which is about half the number of texts required by uniform sampling from the population to achieve similar error. These results suggest that LS sampling and KL sampling can achieve comparable estimation accuracy with about half the number of unique texts by selecting important texts.

4.2 Stability of Model Map under Resampling

For both analyses below, we resample n texts with replacement from D_N , resulting in d unique texts. Model coordinates are computed from log-likelihoods over the sampled texts and visualized using t-SNE. See Appendix B for details.

⁴In Uniform resampling, weighting according to the number of duplicates slightly degrades performance.

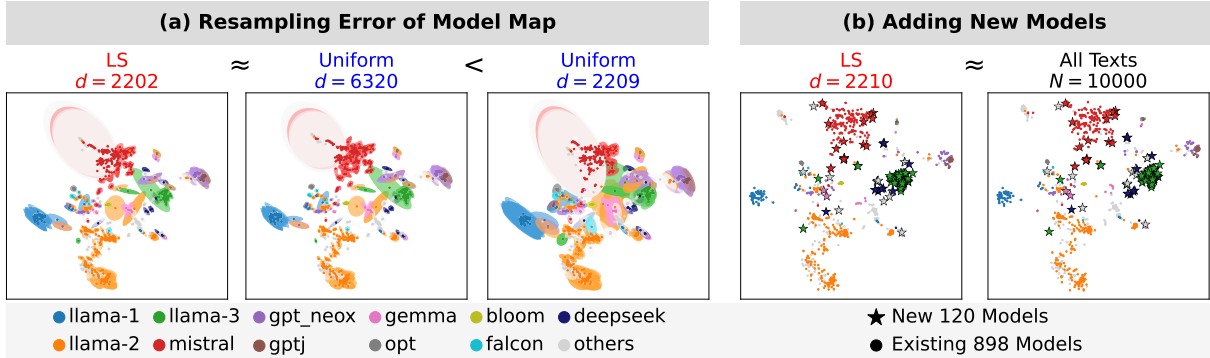


Figure 3: **(a)** Model maps based on LS ($n = 2900$, $d = 2202$), uniform ($n = 10000$, $d = 6320$), and uniform ($n = 2500$, $d = 2209$) sampling. Each map shows the mean coordinates and their variability as ellipses across 100 trials. **(b)** Model maps with 120 new models added to existing 898 models. The left panel uses $d = 2210$ unique texts selected by LS sampling with $n = 2900$. The right panel uses all $N = 10,000$ texts.

(a) Resampling Error of Model Map. To evaluate variability due to resampling, we repeated the process 100 times per setting. Here, d denotes the average number of unique texts across trials. Figure 3(a) shows three model maps; ellipses indicate the standard deviation of model positions. The first two maps show similar stability, indicating that LS achieves uniform-level robustness with fewer texts. When d is matched, LS still yields lower variability than uniform sampling.

(b) Adding New Models. We tested whether a small set of texts selected by LS sampling is sufficient for placing new models. From 898 models created before April 10, 2024, we sampled $n = 2900$ texts via LS, resulting in $d = 2210$ unique texts⁵. The remaining 120 models were treated as new additions. This setting uses a single resampling trial, so d is the actual number of unique texts. We computed log-likelihoods using only these texts and visualized the updated map. As shown in Fig. 3(b), the result closely matches the full map based on all $N = 10,000$ texts, indicating that reliable placement is achievable with a small subset.

4.3 Prediction of Downstream Performance

Following Oyama et al. (2025), we used model coordinates based on d unique texts to predict the average performance on six downstream tasks (Fig. 4). Although the resampling methods differ in KL estimation, prediction performance is similar across methods, suggesting that the resulting coordinates span comparable subspaces. At $d = 1000$,

⁵Model creation dates were obtained using the Hugging Face’s API.

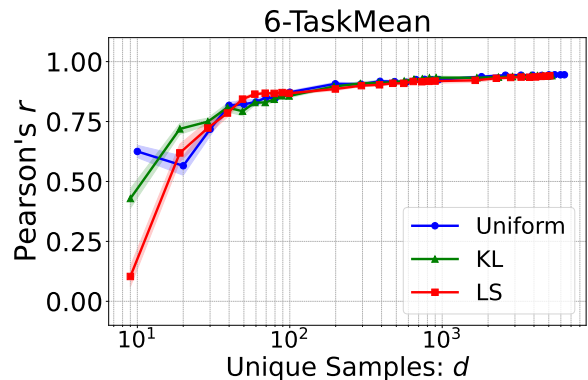


Figure 4: Pearson’s correlation r between predicted and actual scores on the average of six downstream tasks, shown as a function of the number of unique texts d .

all methods achieve $r \approx 0.92$ – 0.93 , indicating that a relatively small number of texts suffices for accurate prediction. See Appendix F for details.

5 Conclusion

We discussed text selection methods to reduce the computational cost of calculating model maps. Experimental results showed that, compared to uniform random sampling, our proposed methods can achieve comparable estimation error with approximately half the number of texts. Furthermore, we confirmed that a small set of texts selected by this resampling is also effective when adding new models to an existing model map. These results enable more efficient comparative analysis of large-scale language models.

Limitations

- The aspect of data sampling remains unexplored. Future investigation is required to understand the extent to which the discussions in this study apply to datasets different from the D_N used in this study.
- Regarding the experiments for adding new models, we did not include a detailed discussion on the number or types of the new models added.
- While LS and KL sampling both outperformed uniform sampling in KL divergence estimation, the difference disappeared in downstream performance prediction, where all methods performed similarly. This suggests that improvements in distance estimation do not necessarily lead to gains in downstream utility, and the relationship between the two warrants further investigation.

Acknowledgments

This study was partially supported by JSPS KAKENHI 22H05106, 23H03355, JST CREST JPMJCR21N3, JST BOOST JPMJBS2407.

References

- Edward Beeching, Clémentine Fourier, Nathan Habib, Sheon Han, Nathan Lambert, Nazneen Rajani, Omar Sanseviero, Lewis Tunstall, and Thomas Wolf. 2023. Open LLM Leaderboard. https://huggingface.co/spaces/open-llm-leaderboard-old/open_llm_leaderboard.
- Peter J Bickel and Anat Sakov. 2008. On the Choice of m in the m out of n Bootstrap and Confidence Bounds for Extrema. *Statistica Sinica*, pages 967–985.
- Peter Clark, Isaac Cowhey, Oren Etzioni, Tushar Khot, Ashish Sabharwal, Carissa Schoenick, and Oyvind Tafjord. 2018. [Think you have Solved Question Answering? Try ARC, the AI2 Reasoning Challenge](#). *Preprint*, arXiv:1803.05457.
- Karl Cobbe, Vineet Kosaraju, Mohammad Bavarian, Mark Chen, Heewoo Jun, Lukasz Kaiser, Matthias Plappert, Jerry Tworek, Jacob Hilton, Reiichiro Nakano, Christopher Hesse, and John Schulman. 2021. [Training Verifiers to Solve Math Word Problems](#). *Preprint*, arXiv:2110.14168.
- Petros Drineas and Ravi Kannan. 2001. [Fast Monte-Carlo Algorithms for Approximate Matrix Multiplication](#). In *Proceedings 42nd IEEE Symposium on Foundations of Computer Science*, pages 452–459.
- B. Efron and R.J. Tibshirani. 1994. *An Introduction to the Bootstrap*. Chapman & Hall/CRC Monographs on Statistics & Applied Probability. Taylor & Francis.
- Leo Gao, Stella Biderman, Sid Black, Laurence Golding, Travis Hoppe, Charles Foster, Jason Phang, Horace He, Anish Thite, Noa Nabeshima, Shawn Presser, and Connor Leahy. 2020. [The Pile: An 800GB Dataset of Diverse Text for Language Modeling](#). *Preprint*, arXiv:2101.00027.
- Dan Hendrycks, Collin Burns, Steven Basart, Andy Zou, Mantas Mazeika, Dawn Song, and Jacob Steinhardt. 2021. [Measuring Massive Multitask Language Understanding](#). *Preprint*, arXiv:2009.03300.
- Stephanie Lin, Jacob Hilton, and Owain Evans. 2022. [TruthfulQA: Measuring How Models Mimic Human Falsehoods](#). *Preprint*, arXiv:2109.07958.
- Momose Oyama, Hiroaki Yamagiwa, Yusuke Takase, and Hidetoshi Shimodaira. 2025. [Mapping 1,000+ Language Models via the Log-Likelihood Vector](#). *Preprint*, arXiv:2502.16173.
- Keisuke Sakaguchi, Ronan Le Bras, Chandra Bhagavatula, and Yejin Choi. 2019. [WinoGrande: An Adversarial Winograd Schema Challenge at Scale](#). *Preprint*, arXiv:1907.10641.
- Peter H. Schönemann. 1966. A Generalized Solution of the Orthogonal Procrustes Problem. *Psychometrika*, 31:1–10.
- Hidetoshi Shimodaira. 2014. Higher-Order Accuracy of Multiscale-Double Bootstrap for Testing Regions. *Journal of Multivariate Analysis*, 130:208–223.
- Laurens van der Maaten and Geoffrey Hinton. 2008. [Visualizing Data using t-SNE](#). *Journal of Machine Learning Research*, 9(86):2579–2605.
- Gaël Varoquaux, Lars Buitinck, Gilles Louppe, Olivier Grisel, Fabian Pedregosa, and Andreas Mueller. 2015. [Scikit-learn: Machine Learning Without Learning the Machinery](#). *GetMobile Mob. Comput. Commun.*, 19(1):29–33.
- Robert S. Yuill. 1971. [The Standard Deviational Ellipse; An Updated Tool for Spatial Description](#). *Geografiska Annaler: Series B, Human Geography*, 53(1):28–39.
- Rowan Zellers, Ari Holtzman, Yonatan Bisk, Ali Farhadi, and Yejin Choi. 2019. [HellaSwag: Can a Machine Really Finish Your Sentence?](#) *Preprint*, arXiv:1905.07830.

A Author Contributions

M.O. conceived the overall research idea of reducing computational cost via resampling, developed the LS sampling algorithm using matrix approximation techniques, and implemented all resampling methods and experiments related to model distance

estimation and map construction. R.K. proposed the KL sampling method and proved its optimality. H.S. developed the statistical framework for analyzing sampling and resampling errors, and provided theoretical justification. H.Y. conducted the experiments on downstream task performance prediction. All authors contributed to writing the manuscript. M.O. coordinated the writing process and took the lead on the overall composition, while each author wrote the parts corresponding to their contributions. The project was supervised by M.O. and H.S.

B Details of Model Map Construction

B.1 Log-Likelihood Data of Language Models

In our experiment, we used log-likelihood data (Oyama et al., 2025)⁶ for $K = 1,018$ language models, calculated on $N = 10,000$ texts extracted from the Pile (Gao et al., 2020).

In the experiment described in Section 4.2 for adding new models to the model map, we clipped the log-likelihood matrix L of the existing 898 models at the lower 2nd percentile value -1495.9 , following Oyama et al. (2025). The log-likelihood values of the newly added 120 models were also clipped using -1495.9 as the threshold.

B.2 Visualization of Model Map

This section details the procedure for generating the t-SNE (van der Maaten and Hinton, 2008) visualizations and standard deviational ellipses presented in Fig. 1 and Fig. 3.

Coordinate Computation. Resampling method and the number of texts to resample, n , are chosen. Based on the unique resampled texts D_d^* , the model coordinates $\tilde{Q}_d \in \mathbb{R}^{K \times d}$ are computed. These d dimensional coordinates \tilde{Q}_d are subsequently reduced to two dimensions using the t-SNE algorithm. This entire process, from resampling to t-SNE, is repeated $R = 100$ times to assess variability. For consistency across these R trials, the ‘random_state’ parameter of the t-SNE algorithm is fixed to 42. The initial coordinates for t-SNE in each trial are determined by applying PCA to the \tilde{Q}_d matrix calculated for that specific trial.

Coordinate Alignment. Let $\mathbf{X}_r \in \mathbb{R}^{K \times 2}$ denote the matrix of t-SNE coordinates obtained from the r -th trial (for $r = 1, \dots, R$), and \mathbf{X}_{ref} as the t-SNE coordinates of \mathbf{Q} . Since t-SNE results can vary due to inherent translational and rotational

ambiguities, an alignment procedure is necessary to compare the R sets of coordinates. First, each set of coordinates \mathbf{X}_r is centered by subtracting its mean: $\mathbf{Y}_r := \mathbf{X}_r - \bar{\mathbf{X}}_r$. Next, the Orthogonal Procrustes (Schönemann, 1966) analysis is applied to align these centered coordinate sets. For each subsequent set \mathbf{Y}_r (where $r = 1, \dots, R$), an orthogonal transformation matrix \mathbf{U}_r is found that best aligns \mathbf{Y}_r with $\mathbf{Y}_{\text{ref}} = \mathbf{X}_{\text{ref}} - \bar{\mathbf{X}}_{\text{ref}}$. The aligned coordinates are then given by $\mathbf{Z}_r := \mathbf{Y}_r \mathbf{U}_r$.

Centrography. After aligning all $R = 100$ sets of t-SNE coordinates \mathbf{Z}_r , the mean coordinate $\bar{z}_i \in \mathbb{R}^2$ and the covariance matrix $\text{Cov}(z_i) \in \mathbb{R}^{2 \times 2}$ are calculated for each model i across the R trials. The standard deviational ellipses (Yuill, 1971) shown in the figures are derived from these covariance matrices, with their height, width, and angle determined by the eigenvalues and eigenvectors of $\text{Cov}(z_i)$.

C KL Sampling

Notation. We resample a text x_s from the dataset $D_N = \{x_1, \dots, x_N\}$ with probability π_s . Let the n resampled texts be denoted by $\{x_{u_1}, \dots, x_{u_n}\}$. Define $\tilde{\mathbf{Q}} = (Q^{(u_1)}, \dots, Q^{(u_n)}) \in \mathbb{R}^{K \times n}$, and $\tilde{q}_i \in \mathbb{R}^n$ as the i -th row vector of $\tilde{\mathbf{Q}}$. Denoting the (i, t) -th element of $\tilde{\mathbf{Q}}$ as $\tilde{q}_i(x_{u_t})$, we see that this value is equal to $q_i(x_{u_t})$. Note that, unlike the notation used in Section 3.2, \tilde{q} allows for duplication of the resampled texts and its columns are resampled from the double-centered matrix \mathbf{Q} .

Let $\mathbf{w}_n = (1/n\pi_{u_1}, \dots, 1/n\pi_{u_n})^\top \in \mathbb{R}^n$ be the weights on the resampled texts, and let $\mathbf{W} = \text{diag}(\mathbf{w}_n)$ be the corresponding diagonal matrix. Define $g_{ij} = \|\mathbf{q}_i - \mathbf{q}_j\|^2$ and $\tilde{g}_{ij} = \|\tilde{q}_i - \tilde{q}_j\|_{\mathbf{w}_n}$, where the weighted norm is taken with respect to \mathbf{w}_n .

LS Sampling. According to Drineas and Kanthan (2001), the expected Frobenius norm of the approximation error $\mathbb{E} \left[\|\tilde{\mathbf{Q}} \mathbf{W} \tilde{\mathbf{Q}}^\top - \mathbf{Q} \mathbf{Q}^\top\|_F^2 \right]$ is minimized when the resampling probabilities satisfy $\pi_s \propto \|Q^{(s)}\|^2$.

KL sampling (Proposed). Instead of approximating the inner products in \mathbf{Q} , we aim to approximate the sum of the pairwise distances. We prove that the resampling probabilities π_s that minimize $\mathbb{E} \left[\sum_{i,j=1}^K (\tilde{g}_{ij} - g_{ij})^2 \right]$ are given by

$$\pi_s \propto \sqrt{\sum_{i,j=1}^K (q_i(x_s) - q_j(x_s))^4}.$$

⁶<https://github.com/shimo-lab/modelmap>

Lemma 1. For any $i, j \in \{1, \dots, K\}$, it holds that

$$\mathbb{E}[\tilde{g}_{ij}] = g_{ij}.$$

Proof.

$$\begin{aligned} & \mathbb{E}[\tilde{g}_{ij}] \\ &= \mathbb{E}[\|\tilde{\mathbf{q}}_i - \tilde{\mathbf{q}}_j\|_{\mathbf{w}_n}^2] \\ &= \mathbb{E}\left[\sum_{t=1}^n \frac{1}{n\pi_{u_t}} (\tilde{q}_i(x_{u_t}) - \tilde{q}_j(x_{u_t}))^2\right] \\ &= \frac{1}{n} \sum_{t=1}^n \mathbb{E}\left[\frac{1}{\pi_{u_t}} (q_i(x_{u_t}) - q_j(x_{u_t}))^2\right] \\ &= \frac{1}{n} \sum_{t=1}^n \sum_{s=1}^N \frac{1}{\pi_s} (q_i(x_s) - q_j(x_s))^2 \pi_s \\ &= \|\mathbf{q}_i - \mathbf{q}_j\|^2 \\ &= g_{ij}. \end{aligned}$$

□

Lemma 2. The variance of the weighted distance after resampling is given by

$$\begin{aligned} & \text{Var}(\tilde{g}_{ij}) \\ &= \frac{1}{n} \sum_{s=1}^N \frac{1}{\pi_s} (q_i(x_s) - q_j(x_s))^4 - \frac{1}{n} \|\mathbf{q}_i - \mathbf{q}_j\|^4. \end{aligned}$$

Proof. Noting that the resampling is performed independently, we obtain

$$\begin{aligned} & \text{Var}(\tilde{g}_{ij}) \\ &= \text{Var}\left(\sum_{t=1}^n \frac{1}{n\pi_{u_t}} (\tilde{q}_i(x_{u_t}) - \tilde{q}_j(x_{u_t}))^2\right) \\ &= \sum_{t=1}^n \text{Var}\left(\frac{1}{n\pi_{u_t}} (\tilde{q}_i(x_{u_t}) - \tilde{q}_j(x_{u_t}))^2\right) \\ &= \sum_{t=1}^n \left(\frac{1}{n^2} \sum_{s=1}^N \frac{1}{\pi_s} (q_i(x_s) - q_j(x_s))^4 - \frac{1}{n^2} \|\mathbf{q}_i - \mathbf{q}_j\|^4\right) \\ &= \frac{1}{n} \sum_{s=1}^N \frac{1}{\pi_s} (q_i(x_s) - q_j(x_s))^4 - \frac{1}{n} \|\mathbf{q}_i - \mathbf{q}_j\|^4. \end{aligned}$$

□

Proposition 1. The resampling probabilities π_s that minimize $\mathbb{E}\left[\sum_{i,j=1}^K (\tilde{g}_{ij} - g_{ij})^2\right]$ are given by

$$\pi_s \propto \sqrt{\sum_{i,j=1}^K (q_i(x_s) - q_j(x_s))^4}.$$

Proof. By Lemma 1, we have

$$\mathbb{E}\left[\sum_{i,j=1}^K (\tilde{g}_{ij} - g_{ij})^2\right] = \sum_{i,j=1}^K \text{Var}(\tilde{g}_{ij}).$$

Therefore, by Lemma 2, we aim to minimize

$$f(\pi_1, \dots, \pi_N) = \sum_{i,j=1}^K \sum_{s=1}^N \frac{1}{\pi_s} (q_i(x_s) - q_j(x_s))^4$$

subject to the constraint $\sum_{s=1}^N \pi_s = 1$. Let

$$\begin{aligned} & g(\pi_1, \dots, \pi_N, \lambda) \\ &= f(\pi_1, \dots, \pi_N) + \lambda \left(\sum_{s=1}^N \pi_s - 1\right). \end{aligned}$$

By setting $\frac{\partial g}{\partial \pi_s} = 0$, we obtain

$$\lambda \pi_s^2 = \sum_{i,j=1}^K (q_i(x_s) - q_j(x_s))^4.$$

Using the condition $\sum_{s=1}^N \pi_s = 1$, it follows that

$$\sqrt{\lambda} = \sum_{s=1}^N \sqrt{\sum_{i,j=1}^K (q_i(x_s) - q_j(x_s))^4}.$$

Therefore, we have

$$\pi_s = \frac{\sqrt{\sum_{i,j=1}^K (q_i(x_s) - q_j(x_s))^4}}{\sum_{s'=1}^N \sqrt{\sum_{i,j=1}^K (q_i(x_{s'}) - q_j(x_{s'}))^4}}.$$

□

D Error Evaluation without Normalization

In Section 4.1, the error was normalized by the magnitude of KL divergence for each model pair to evaluate the relative error with respect to KL divergence. In this section, we evaluate the error without normalization for each model pair. The errors \tilde{e}_{ij} and e_{ij}^\dagger are redefined by focusing on the sum of squared differences.

$$\tilde{e}_{ij} = \frac{\tilde{g}_{ij} - g_{ij}}{C}, \quad e_{ij}^\dagger = \frac{g_{ij} - g_{ij}^\dagger}{C^\dagger},$$

where

$$C = \frac{1}{K^2} \sum_{i,j=1}^K g_{ij}, \quad C^\dagger = \frac{1}{K^2} \sum_{i,j=1}^K g_{ij}^\dagger.$$

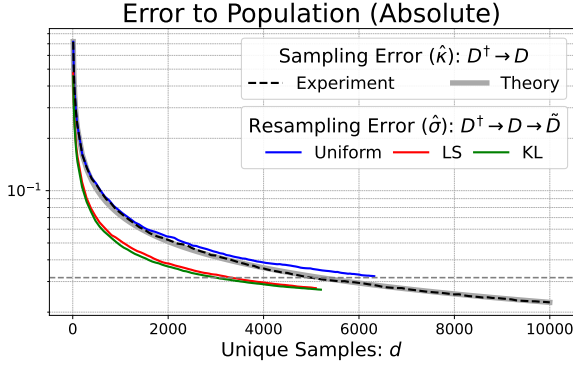


Figure 5: Result of error evaluation without normalization for each model pair. Other settings are the same as Fig. 2.

In the KL sampling method derived in Appendix C, optimization is performed to reduce $\mathbb{E}[\sum_{i,j=1}^K (\tilde{g}_{ij} - g_{ij})^2 \mid D_N]$, which corresponds to minimizing the sum of absolute squared errors.

The results of evaluating the error are shown in Fig. 5. KL sampling indeed has a slightly smaller error than LS sampling under this evaluation. On the other hand, in Fig. 2, LS sampling can have a slightly smaller error than KL sampling. In both plots, the performance difference between LS sampling and KL sampling is very small. Therefore, this paper primarily explains the simpler LS sampling method due to its comparable performance.

E Estimating the Population Error of Resampled Distances

This section provides a detailed discussion of the error evaluation method introduced in Section 4.1.

Sampling Error. We consider the case where a dataset $D_n = (x_1, \dots, x_n)$ of size n is sampled from a large population of texts $D^\dagger = (x_1^\dagger, \dots, x_{N_0}^\dagger)$. We assume that $N_0 \gg n$ and n is sufficiently large. Let $L^\dagger \in \mathbb{R}^{K \times N_0}$ and $L \in \mathbb{R}^{K \times n}$ denote the log-likelihood matrices evaluated on D^\dagger and D_n , respectively. Their doubly centered versions are denoted by $Q^\dagger = [Q^{\dagger(1)}, \dots, Q^{\dagger(N_0)}]$ and $Q = [Q^{(1)}, \dots, Q^{(n)}]$, with row vectors $q_i^\dagger \in \mathbb{R}^{N_0}$ and $q_i \in \mathbb{R}^n$ representing the coordinates of model p_i in each case. When n is sufficiently large, the average vector used in centering Q can be well approximated by that of Q^\dagger , and thus each column of Q may be regarded as a random sample (without replacement) from the columns of Q^\dagger .

We focus on the squared Euclidean distance between two models p_i and p_j . To ensure comparabil-

ity with the case where the data size is $n = N$, we introduce a scaling factor to normalize the estimate and define:

$$\begin{aligned} g_{ij} &= \frac{N}{n} \|q_i - q_j\|^2 \\ &= \frac{N}{n} \sum_{s=1}^n (q_i(x_s) - q_j(x_s))^2, \\ g_{ij}^\dagger &= \frac{N}{N_0} \|q_i^\dagger - q_j^\dagger\|^2 \\ &= \frac{N}{N_0} \sum_{s=1}^{N_0} (q_i^\dagger(x_s^\dagger) - q_j^\dagger(x_s^\dagger))^2. \end{aligned}$$

We define the sampling error as

$$\varepsilon_{ij} = g_{ij} - g_{ij}^\dagger.$$

Since the terms $\{(q_i(x_s) - q_j(x_s))^2\}_{s=1}^n$ can be regarded as random samples from $\{(q_i^\dagger(x_s^\dagger) - q_j^\dagger(x_s^\dagger))^2\}_{s=1}^{N_0}$, g_{ij} is an unbiased estimator of g_{ij}^\dagger , and thus the sampling error satisfies $\mathbb{E}[\varepsilon_{ij}] = 0$.

The mean squared error (MSE) of this sampling error is then given by

$$\kappa_{ij,n}^2 = \mathbb{E}[\varepsilon_{ij}^2].$$

Following the formulation in Section 4.1, we define the aggregated sampling MSE as

$$\kappa_n^2 = \frac{1}{K^2} \sum_{i,j=1}^K \frac{\kappa_{ij,n}^2}{\max(g_{ij}^\dagger, \varepsilon_0)^2},$$

where $\varepsilon_0 > 0$ is a small constant to avoid division by zero.

Bootstrap Estimate of Sampling Error. We consider a bootstrap procedure that randomly samples n texts uniformly with replacement from the dataset D_n (we note that D_n may later be replaced by D_N). That is, each text in D_n is selected with equal probability $\pi_s = 1/n$. Let $\tilde{D}_n = (\tilde{x}_1, \dots, \tilde{x}_n)$ denote the resampled dataset. The log-likelihood matrix and its doubly centered version for \tilde{D}_n are denoted by $\tilde{L} \in \mathbb{R}^{K \times n}$ and $\tilde{Q} \in \mathbb{R}^{K \times n} = [\tilde{Q}^{(1)}, \dots, \tilde{Q}^{(n)}]$, respectively, and the coordinate vector of model p_i is denoted by $\tilde{q}_i \in \mathbb{R}^n$. When n is sufficiently large, the mean vector used for centering \tilde{Q} can be well approximated by that of Q , so each column of \tilde{Q} may be regarded as a random sample (with replacement) from the columns of Q .

Unlike in Section 3.2, where resampling with replacement was handled by recording the number

of duplicates and incorporating them as weights, we here represent the resampled data explicitly by allowing duplicate entries in the coordinate vectors $\tilde{\mathbf{q}}_i$. Thus, the difference is only notational, and both approaches describe the same underlying resampling process.

As in the previous subsection, we focus on the squared Euclidean distance between models p_i and p_j . To ensure comparability with the case of dataset size $n = N$, we scale the estimate as follows:

$$\begin{aligned}\tilde{g}_{ij} &= \frac{N}{n} \|\tilde{\mathbf{q}}_i - \tilde{\mathbf{q}}_j\|^2 \\ &= \frac{N}{n} \sum_{s=1}^n (\tilde{q}_i(\tilde{x}_s) - \tilde{q}_j(\tilde{x}_s))^2.\end{aligned}$$

The terms $\{(\tilde{q}_i(\tilde{x}_s) - \tilde{q}_j(\tilde{x}_s))^2\}_{s=1}^n$ can be viewed as a bootstrap sample drawn (with replacement) from the set $\{(q_i(x_s) - q_j(x_s))^2\}_{s=1}^n$. We define the resampling error as

$$\tilde{\varepsilon}_{ij} = \tilde{g}_{ij} - g_{ij},$$

which satisfies $\mathbb{E}[\tilde{\varepsilon}_{ij} \mid D_n] = 0$ by construction. The conditional mean squared error (MSE) of \tilde{g}_{ij} given D_n is defined as

$$\tau_{ij,n}^2 = \mathbb{E}[\tilde{\varepsilon}_{ij}^2 \mid D_n].$$

In practice, we estimate this quantity by performing R independent bootstrap trials and computing

$$\tau_{ij,n}^2 = \frac{1}{R} \sum_{r=1}^R \left(\tilde{\varepsilon}_{ij}^{(r)}\right)^2,$$

where $\tilde{\varepsilon}_{ij}^{(r)}$ is the resampling error from the r -th trial.

This quantity $\tau_{ij,n}^2$ serves as the bootstrap estimate of $\kappa_{ij,n}^2$ (Efron and Tibshirani, 1994):

$$\hat{\kappa}_{ij,n}^2 = \tau_{ij,n}^2.$$

We may also replace D_n with D_N ; in that case, this procedure corresponds to an n -out-of- N bootstrap (Bickel and Sakov, 2008), and $\tau_{ij,n}^2$ remains a valid estimator of $\kappa_{ij,n}^2$ (Shimodaira, 2014). Moreover, the resampling MSE obeys a standard scaling law $\tau_{ij,n}^2 \propto n^{-1}$, and can be approximated by the theoretical relation

$$\tau_{ij,n}^2 = \frac{N}{n} \tau_{ij,N}^2.$$

Following Section 4.1, we define the aggregated resampling MSE as

$$\tau_{\text{unif},n}^2 = \frac{1}{K^2} \sum_{i,j=1}^K \frac{\tau_{ij,n}^2}{\max(g_{ij}, \varepsilon_0)^2}.$$

This corresponds to the uniform resampling case discussed in Section 4.1. The above discussion on $\tau_{ij,n}^2$ also applies directly to $\tau_{\text{unif},n}^2$, and we obtain the bootstrap estimate of the sampling MSE κ_n^2 as

$$\hat{\kappa}_n^2 = \tau_{\text{unif},n}^2.$$

Theoretical scaling gives the approximation

$$\tau_{\text{unif},n}^2 = \frac{N}{n} \tau_{\text{unif},N}^2.$$

Decomposition of Population Error. We consider a two-stage sampling procedure: first, we obtain a dataset D_N by randomly sampling N texts from the population D^\dagger ; then, we perform weighted resampling with replacement from D_N to obtain a smaller dataset \tilde{D}_n of size n . As described in Section 3, we consider three types of resampling weights: LS sampling, KL sampling, and uniform sampling.

The estimated squared distance based on the resampled data is defined as

$$\tilde{g}_{ij} = \|\tilde{\mathbf{q}}_i - \tilde{\mathbf{q}}_j\|_{\mathbf{w}_d}^2,$$

where the notation already includes the scaling factor N/n through the weights. In particular, for uniform sampling, we have $\pi_s = 1/N$, which leads to the weight $1/(n\pi_s) = N/n$.

We analyze the error of the resampling estimator \tilde{g}_{ij} relative to the true value g_{ij}^\dagger in the population. Define the error as

$$\varepsilon_{ij}^\dagger = \tilde{g}_{ij} - g_{ij}^\dagger.$$

This error can be decomposed as

$$\begin{aligned}\varepsilon_{ij}^\dagger &= (\tilde{g}_{ij} - g_{ij}) + (g_{ij} - g_{ij}^\dagger) \\ &= \tilde{\varepsilon}_{ij} + \varepsilon_{ij},\end{aligned}$$

where $\tilde{\varepsilon}_{ij}$ and ε_{ij} denote the resampling error and the sampling error, respectively.

Taking the expectation of the squared error, we obtain the decomposition of the MSE:

$$\begin{aligned}\sigma_{ij}^2 &= \mathbb{E}[(\varepsilon_{ij}^\dagger)^2] \\ &= \mathbb{E}[(\tilde{\varepsilon}_{ij} + \varepsilon_{ij})^2] \\ &= \mathbb{E}[\mathbb{E}[\tilde{\varepsilon}_{ij}^2 \mid D_N]] \\ &\quad + 2\mathbb{E}[\mathbb{E}[\tilde{\varepsilon}_{ij} \mid D_N]\varepsilon_{ij}] + \mathbb{E}[\varepsilon_{ij}^2] \\ &= \mathbb{E}[\tau_{ij,n}^2] + \kappa_{ij,N}^2,\end{aligned}$$

where we used $\mathbb{E}[\tilde{\varepsilon}_{ij} | D_N] = 0$.

Here, $\tau_{ij,n}^2$ is computed from resampling errors $\tilde{\varepsilon}_{ij}^{(r)}$ obtained via weighted resampling from D_N . The term $\kappa_{ij,N}^2$ can be estimated by the bootstrap MSE under uniform resampling of size N , denoted by $\tau_{ij,\text{unif},N}^2$. Thus, we estimate σ_{ij}^2 by

$$\hat{\sigma}_{ij}^2 = \tau_{ij,n}^2 + \tau_{ij,\text{unif},N}^2.$$

As in Section 4.1, we define the aggregated population MSE by

$$\sigma_n^2 = \frac{1}{K^2} \sum_{i,j=1}^K \frac{\sigma_{ij,n}^2}{\max(g_{ij}^\dagger, \varepsilon_0)^2}.$$

Substituting the estimate $\hat{\sigma}_{ij}^2$ into this expression yields the estimate of σ_n^2 :

$$\hat{\sigma}_n^2 = \tau_n^2 + \tau_{\text{unif},N}^2.$$

F Model Performance Prediction

We computed the log-likelihoods of the unique texts contained in the resampled data and, following Oyama et al. (2025), used these values to predict model performance. This section describes the experiments in detail.

F.1 Model Performance

Following Oyama et al. (2025), we used the Open LLM Leaderboard v1 (Beeching et al., 2023) as the source of model performance scores⁷. The leaderboard provides scores for the following six benchmark tasks⁸: AI2 Reasoning Challenge (ARC) (Clark et al., 2018), HellaSwag (Zellers et al., 2019), MMLU (Hendrycks et al., 2021), TruthfulQA (Lin et al., 2022), Winogrande (Sakaguchi et al., 2019), and GSM8K (Cobbe et al., 2021).

In addition to these benchmark scores, we followed Oyama et al. (2025) and also predicted (i) the average across the six tasks (hereafter referred to as 6-TaskMean) and (ii) the mean log-likelihood $\bar{\ell}_i$ of the log-likelihood vector $\ell_i \in \mathbb{R}^N$.

F.2 Dataset Configuration

The number of resampled texts was set to

$$n \in \{10, 20, \dots, 90, 100, 200, \dots, 900, 1000, 2000, \dots, 9000, 10000\}.$$

⁷https://huggingface.co/spaces/open-llm-leaderboard-old/open_llm_leaderboard

⁸Benchmark scores are available for 996 of the 1,018 models released by Oyama et al. (2025). For convenience, we denote this subset size by K throughout this section.

As explained in Section 3, resampling n texts from D_N yields \tilde{D}_n , and from this resampled set we extract a set of d unique texts, $D_d^* = \{x_{u_1}, \dots, x_{u_d}\}$. Using these d texts, we computed the log-likelihood matrix $\mathbf{L}_d \in \mathbb{R}^{K \times d}$ and then formed the doubly-centered matrix $\tilde{\mathbf{Q}}_d = [\tilde{\mathbf{q}}_1, \dots, \tilde{\mathbf{q}}_K]^\top \in \mathbb{R}^{K \times d}$ with scaling weights $\mathbf{w}_d = \left(\frac{c(u_1)}{n\pi_{u_1}}, \dots, \frac{c(u_d)}{n\pi_{u_d}}\right)^\top \in \mathbb{R}^d$.

For each benchmark task, the dataset is given as $\{(\tilde{\mathbf{q}}_1, f_1), \dots, (\tilde{\mathbf{q}}_K, f_K)\}$, where $\tilde{\mathbf{q}}_i = (\tilde{q}_i(x_{u_1}), \dots, \tilde{q}_i(x_{u_d}))^\top \in \mathbb{R}^d$ is the i -th row of $\tilde{\mathbf{Q}}_d$ corresponding to language model p_i , and $f_i \in [0, 100]$ is its benchmark score.

F.3 Regression Formulation

As in Oyama et al. (2025), we adopted ridge regression to predict each benchmark score. The matrix of explanatory variables is

$$\tilde{\mathbf{Q}}_d \mathbf{W}_d^{1/2} \in \mathbb{R}^{K \times d}, \quad (1)$$

where the diagonal matrix $\mathbf{W}_d^{1/2} \in \mathbb{R}^{d \times d}$ has $\sqrt{\frac{c(u_t)}{n\pi_{u_t}}}$ on its t -th diagonal entry⁹. Let $\mathbf{f} = (f_1, \dots, f_K)^\top \in \mathbb{R}^K$ denote the vector of target variables. The objective function, parameterized by $\boldsymbol{\theta} \in \mathbb{R}^d$, is defined as

$$\mathcal{L}(\boldsymbol{\theta}) = \|\mathbf{f} - \tilde{\mathbf{Q}}_d \mathbf{W}_d^{1/2} \boldsymbol{\theta}\|^2 + \alpha \|\boldsymbol{\theta}\|^2,$$

where $\alpha \in \mathbb{R}_{>0}$ is a hyperparameter controlling the strength of regularization.

F.4 Training Setup

We partitioned the set of models into five folds according to their model types, as defined in Oyama et al. (2025). We then trained the parameters and predicted the benchmark scores. Training was performed with RidgeCV from scikit-learn (Varoquaux et al., 2015). To account for randomness, we repeated the data split with five different random seeds. As the evaluation metric, we computed Pearson’s correlation coefficient (r) between the predicted and true benchmark scores for each split and averaged the results.

⁹We adopt $\tilde{\mathbf{Q}}_d \mathbf{W}_d^{1/2}$ as the matrix of explanatory variables rather than $\tilde{\mathbf{Q}}_d$ itself. Let $\mathbf{W}_d = \text{diag}(\mathbf{w}_d)$, whose t -th diagonal entry is $\frac{c(u_t)}{n\pi_{u_t}}$. Since $\mathbf{W}_d^{1/2} \mathbf{W}_d^{1/2} = \mathbf{W}_d$, we have $\tilde{\mathbf{Q}}_d \mathbf{W}_d^{1/2} (\tilde{\mathbf{Q}}_d \mathbf{W}_d^{1/2})^\top = \tilde{\mathbf{Q}}_d \mathbf{W}_d \tilde{\mathbf{Q}}_d^\top$. Then Lemma 1 of Drineas and Kannan (2001) gives $\mathbb{E}[\tilde{\mathbf{Q}}_d \mathbf{W}_d \tilde{\mathbf{Q}}_d^\top] = \mathbf{Q} \mathbf{Q}^\top$. Thus, pre-multiplying by $\mathbf{W}_d^{1/2}$ preserves this desirable expectation while appropriately re-scaling the features.

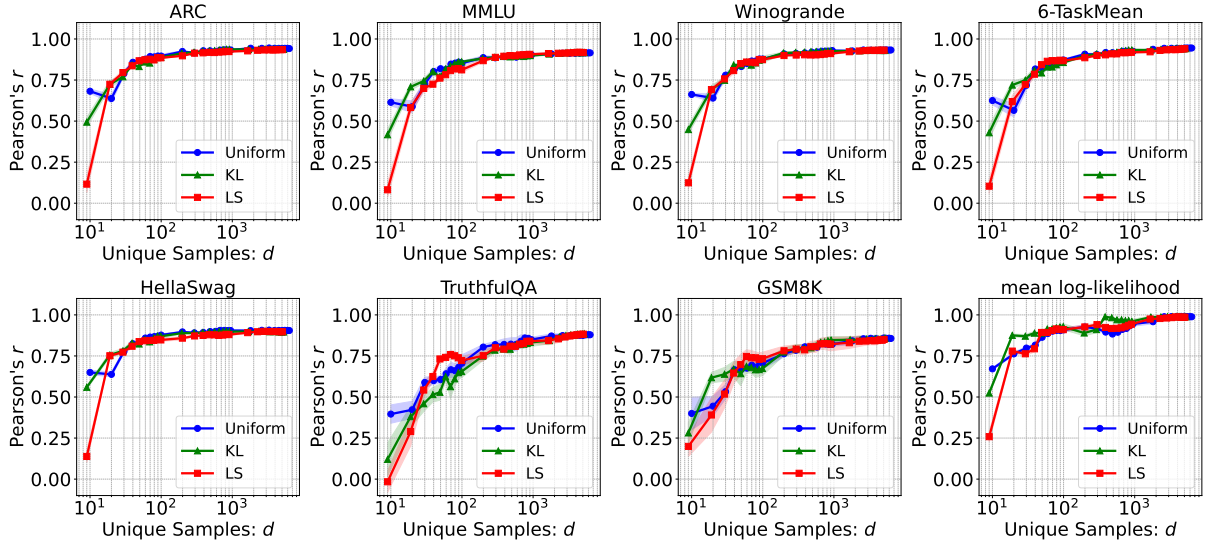


Figure 6: Pearson’s correlation coefficient (r) between the predicted scores and the benchmark scores as a function of the number of unique texts d (determined by the resampling size n), plotted separately for each resampling method. Solid lines indicate the mean across five different data splits, and the shaded bands show ± 1 standard deviation. For every task and every method, predictive performance improves as d increases.

| n | d | Method | ARC | HellaSwag | MMLU | TruthfulQA | Winogrande | GSM8K | 6-TaskMean | mean log-likelihood |
|--------|------|---------|-------------------|-------------------|-------------------|--------------------|-------------------|-------------------|-------------------|---------------------|
| 10^1 | 10 | Uniform | 0.682 ± 0.014 | 0.650 ± 0.014 | 0.614 ± 0.022 | 0.396 ± 0.056 | 0.662 ± 0.008 | 0.400 ± 0.099 | 0.625 ± 0.026 | 0.671 ± 0.007 |
| | 9 | KL | 0.494 ± 0.029 | 0.559 ± 0.010 | 0.417 ± 0.034 | 0.120 ± 0.101 | 0.448 ± 0.025 | 0.281 ± 0.063 | 0.429 ± 0.041 | 0.524 ± 0.012 |
| | 9 | LS | 0.116 ± 0.051 | 0.138 ± 0.036 | 0.082 ± 0.045 | -0.016 ± 0.065 | 0.124 ± 0.040 | 0.199 ± 0.061 | 0.104 ± 0.043 | 0.258 ± 0.030 |
| 10^2 | 100 | Uniform | 0.896 ± 0.012 | 0.877 ± 0.007 | 0.852 ± 0.012 | 0.705 ± 0.052 | 0.878 ± 0.007 | 0.706 ± 0.034 | 0.872 ± 0.006 | 0.909 ± 0.010 |
| | 99 | KL | 0.888 ± 0.012 | 0.870 ± 0.015 | 0.861 ± 0.006 | 0.655 ± 0.036 | 0.875 ± 0.021 | 0.674 ± 0.043 | 0.857 ± 0.008 | 0.928 ± 0.018 |
| | 99 | LS | 0.885 ± 0.005 | 0.847 ± 0.008 | 0.812 ± 0.016 | 0.722 ± 0.023 | 0.874 ± 0.009 | 0.733 ± 0.039 | 0.868 ± 0.006 | 0.910 ± 0.012 |
| 10^3 | 949 | Uniform | 0.933 ± 0.004 | 0.905 ± 0.005 | 0.903 ± 0.007 | 0.849 ± 0.015 | 0.929 ± 0.004 | 0.821 ± 0.012 | 0.925 ± 0.005 | 0.946 ± 0.014 |
| | 912 | KL | 0.937 ± 0.003 | 0.898 ± 0.006 | 0.899 ± 0.010 | 0.832 ± 0.025 | 0.926 ± 0.002 | 0.847 ± 0.022 | 0.933 ± 0.007 | 0.960 ± 0.012 |
| | 898 | LS | 0.923 ± 0.003 | 0.880 ± 0.004 | 0.906 ± 0.007 | 0.840 ± 0.012 | 0.911 ± 0.007 | 0.822 ± 0.041 | 0.919 ± 0.009 | 0.943 ± 0.015 |
| 10^4 | 6335 | Uniform | 0.942 ± 0.002 | 0.905 ± 0.004 | 0.916 ± 0.006 | 0.879 ± 0.018 | 0.933 ± 0.005 | 0.857 ± 0.018 | 0.945 ± 0.004 | 0.989 ± 0.006 |
| | 5240 | KL | 0.937 ± 0.002 | 0.896 ± 0.005 | 0.917 ± 0.005 | 0.885 ± 0.009 | 0.930 ± 0.003 | 0.857 ± 0.026 | 0.941 ± 0.005 | 0.988 ± 0.006 |
| | 5080 | LS | 0.935 ± 0.002 | 0.897 ± 0.006 | 0.918 ± 0.007 | 0.882 ± 0.014 | 0.931 ± 0.005 | 0.851 ± 0.019 | 0.941 ± 0.004 | 0.986 ± 0.007 |

Table 2: Summary of the representative values from Fig. 6. For each resampling method, and for $n = 10^1, 10^2, 10^3, 10^4$ (with the corresponding numbers of unique texts d), the table reports Pearson’s correlation r between the predicted and true benchmark scores, together with ± 1 standard deviation.

For each training set (i.e., the four folds in the outer five-fold CV), we conducted an inner five-fold cross-validation to select α from $\{10^1, \dots, 10^9\}$, again following Oyama et al. (2025). The predicted scores were then clipped to the range $[0, 100]$. When the target variable \mathbf{f} was the mean log-likelihood $(\bar{\ell}_1, \dots, \bar{\ell}_K) \in \mathbb{R}^K$, we searched α in $\{10^{-4}, \dots, 10^4\}$ and did not clip the predictions.

E.5 Results

Figure 6 shows Pearson’s correlation coefficient between the predicted scores and the benchmark scores for Uniform, KL, and LS sampling as a function of the number of unique texts d for each resampling size n . Table 2 summarizes representative values obtained for each method at $n = 10^1, 10^2, 10^3, 10^4$ (and the corresponding d).

For all tasks and all methods, Pearson’s correlation coefficient r increases as d grows. As shown in Table 2, even at $d \approx 100$ —for example, for 6-TaskMean—the predicted scores already achieve $r \approx 0.85$ under every resampling method, and only minor differences are observed among the strategies. Hence, predictive performance depends almost solely on the number of unique texts d .

This behavior can be interpreted as follows: when $d \ll K$ ($K \approx 10^3$), the column vectors of $\tilde{Q}_d \mathbf{W}_d^{1/2} \in \mathbb{R}^{K \times d}$ span a subspace of insufficient dimensionality, limiting the expressive power of the regression model. As d increases, the feature space expands and ridge regression becomes effective, leading to a rapid improvement in performance; however, once $d \gtrsim 10^3$ provides sufficient dimensionality, further gains in correlation are gradual.